

Reversible adiabatic temperature change in the shape memory Heusler alloy $\text{Ni}_{2.2}\text{Mn}_{0.8}\text{Ga}$: An effect of structural compatibility


P. Devi,^{1,*} M. Ghorbani Zavareh,¹ C. Salazar Mejía,² K. Hofmann,³ B. Albert,³ C. Felser,¹ M. Nicklas,¹ and Sanjay Singh^{1,4,†}

¹Max Planck Institute for Chemical Physics of Solids, Nöthnitzer Str. 40, 01187 Dresden, Germany

²Dresden High Magnetic Field Laboratory (HLD-EMFL), Helmholtz-Zentrum Dresden-Rossendorf, 01328 Dresden, Germany

³Eduard-Zintl-Institut für Anorganische und Physikalische Chemie, Technische Universität Darmstadt, Alarich-Weiss-Str. 12, 64287 Darmstadt, Germany

⁴School of Materials Science and Technology, Indian Institute of Technology (BHU), Varanasi-221005, India

 (Received 3 May 2018; revised manuscript received 28 September 2018; published 28 December 2018)

The large magnetocaloric effect (MCE) observed in Ni-Mn based shape memory Heusler alloys put them forward to use in magnetic refrigeration technology. It is associated with a first-order magnetostructural (martensitic) phase transition. We conducted a comprehensive study of the MCE for the off-stoichiometric Heusler alloy $\text{Ni}_{2.2}\text{Mn}_{0.8}\text{Ga}$ in the vicinity of its first-order magnetostructural phase transition. We found a reversible MCE under repeated magnetic field cycles. The reversible behavior can be attributed to the small thermal hysteresis of the martensitic phase transition. Based on the analysis of our detailed temperature dependent x-ray diffraction data, we demonstrate the geometric compatibility of the cubic austenite and tetragonal martensite phases. This finding directly relates the reversible MCE behavior to an improved geometric compatibility condition between cubic austenite and tetragonal martensite phases. The approach will help to design shape memory Heusler alloys with a large reversible MCE taking advantage of the first-order martensitic phase transition.

DOI: [10.1103/PhysRevMaterials.2.122401](https://doi.org/10.1103/PhysRevMaterials.2.122401)

The magnetocaloric effect (MCE) can be quantified as an isothermal magnetic entropy change (ΔS_M) or an adiabatic temperature change (ΔT_{ad}) under the application of magnetic field. It is an intrinsic magnetothermodynamic property of magnetic materials [1]. Magnetic refrigeration technology based on the MCE has higher refrigeration efficiency compared to other caloric effects [2] making it an edge over the other technologies. In recent past, different MCE materials have been studied and the potential candidates for magnetic refrigeration are reported as $\text{Gd}_5(\text{Si}_{1-x}\text{Ge}_x)_4$ [3–5], $\text{La}(\text{Fe}_{13-x}\text{Si}_x)$ [6,7], $\text{Mn}(\text{As}_{1-x}\text{Sb}_x)$ [8], $\text{MnFe}(\text{P}_{1-x}\text{As}_x)$ [9], and off-stoichiometric Heusler alloys Ni_2MnX ($X = \text{Ga}, \text{In}, \text{Sb}, \text{and Sn}$) [10–12]. Among these, Ni-Mn-based Heusler alloys are the subject of special interest as they do not involve toxic and rare-earth elements, but exhibit large values of the MCE at a reasonable magnetic field [11–13].

Magnetic shape memory Heusler alloys undergo a first-order structural phase transition from a high temperature, high-symmetry cubic austenite phase to a low temperature, low-symmetry martensite phase [11–17]. This first-order transition leads to large ΔS_M and ΔT_{ad} because of both structural and magnetic contributions to the MCE [11]. For inducing a first-order phase transition, energy must be spent to overcome the potential barrier between the austenite and martensite phases. This energy leads to intrinsic irreversibilities in both ΔS_M and ΔT_{ad} , which can drastically reduce the cooling efficiency of a device. Irreversible behavior arises due to both thermal as well as magnetic hysteresis. To minimize

the irreversibility, it is necessary to reduce the hysteresis [11]. Hysteresis is an inherent property of first-order phase transformation, which can be reduced by various internal parameters such as chemical composition, type and amount of a doping element as well as extrinsic parameters such as the sample preparation method, annealing conditions, applied magnetic field, pressure, heating and cooling rate, sequence of measurements, and cycling [10–14]. Recently, it has been proposed that the reversibility of the phase transition, i.e., small to no hysteresis, can be achieved by satisfying the geometric compatibility condition between austenite and martensite phases [14,18–23].

In the present work, we have studied the MCE and its relation to transformation hysteresis effects at the martensitic transition in the off-stoichiometric shape memory Heusler alloy $\text{Ni}_{2.2}\text{Mn}_{0.8}\text{Ga}$. $\text{Ni}_{2.2}\text{Mn}_{0.8}\text{Ga}$ exhibits a small hysteresis and a conventional MCE, i.e., the temperature increases upon application of a magnetic field. The MCE is reversible in the hysteresis region of the martensitic transformation as our ΔT_{ad} measurements in pulsed magnetic field cycles demonstrate. To investigate the origin of the reversible behavior, we conducted powder x-ray diffraction (PXRD) experiments of the martensite and the austenite phases in order to calculate and analyze the geometric transformation matrix \mathbf{U} . We found a geometric compatibility of both phases in $\text{Ni}_{2.2}\text{Mn}_{0.8}\text{Ga}$. This strongly suggests the geometric compatibility of martensite and austenite phases to be at the basis of only the small hysteresis and the reversible MCE.

A polycrystalline ingot with nominal composition of $\text{Ni}_{2.2}\text{Mn}_{0.8}\text{Ga}$ was prepared under Ar atmosphere from its pure constituent elements using an arc-melting technique. The ingot was melted six times to ensure a good homogeneity.

*parul.devi@cpfs.mpg.de

†sanjay.singh@cpfs.mpg.de

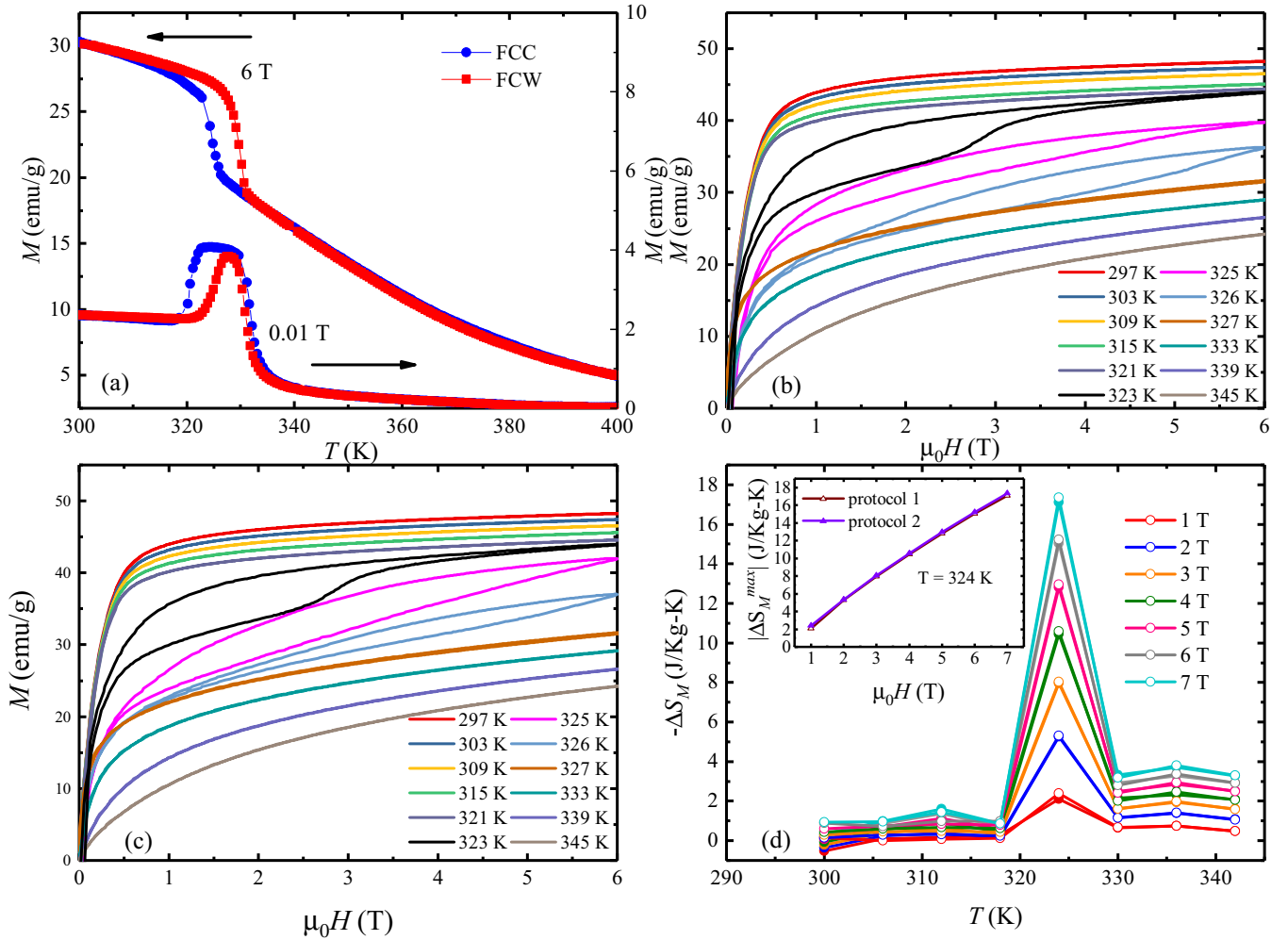


FIG. 1. (a) Field cooled cooling (FCC) and field cooled warming (FCW) magnetization, $M(T)$, curves at 0.01 T and 6 T for Ni_{2.2}Mn_{0.8}Ga. (b) $M(H)$ isotherms with protocol 1 and (c) protocol 2 taken at different temperatures in static magnetic fields up to 6 T between 297 and 345 K. (d) Isothermal magnetic entropy as a function of temperature under different magnetic fields applied, solid and open circles for protocol 1 and 2, respectively. (Inset) Variation of ΔS_M for different magnetic fields at $T = 324$ K for both protocols.

Afterwards, the as-cast button-shaped ingot was annealed for 9 days in a sealed quartz tube under vacuum at 1100 K to obtain high homogeneity and subsequently quenched in an ice-water mixture. The compositional analysis was done by energy-dispersive spectroscopy at different spots. The average composition turns out to be Ni_{2.19}Mn_{0.8}Ga. The magnetic properties have been characterized using a magnetic properties measurement system (Quantum Design). Measurements of the MCE have been carried out in pulsed magnetic fields at the Dresden High Magnetic Field Laboratory using a home-built set up. The powder x-ray diffraction (PXRD) experiments were carried out using a StadiP diffractometer (Stoe & Cie.) with Mo $K_{\alpha 1}$ radiation $\lambda = 0.70930$ Å, Ge [111] monochromator.

The temperature-dependent magnetization curves $M(T)$ of Ni_{2.2}Mn_{0.8}Ga measured in external magnetic fields of 0.01 and 6 T during cooling and heating cycles are shown in Fig. 1. Upon cooling, the austenitic to the martensitic phase transition starts at $M_s = 323$ K (martensite start temperature) and ends at $M_f = 315$ K (martensite finish temperature). Upon heating, the reverse transformation, martensite to austenite, is found to

start at $A_s = 320$ K (austenite start temperature) and to finish at $A_f = 328$ K (austenite finish temperature). The hysteresis width observed from these characteristic temperatures is about 5 K, which is small in comparison with other magnetic shape memory Heusler alloys [12,20,24–27]. $M(T)$ curves at 6 T show that the magnetic fields shift the martensitic transition toward higher temperatures. The magnetic field stabilizes the phase with the higher magnetic moment, in this case, the martensitic phase. Therefore the transition from austenite to martensite can be induced by a field. However, the temperature range at which this transition can be induced is limited by the shift of the transition with the field.

Motivated by the very small thermal hysteresis, we recorded the magnetization data as a function of the magnetic field using two different protocols to determine the magnetic hysteresis. Following protocol 1, the sample was heated up to 400 K to form the austenite phase, then cooled in zero field down to 200 K to ensure the complete transformation into the martensite phase, and then subsequently heated up to the measurement temperature where the $M(H)$ data were taken [see Fig. 1(b)] [28,29]. In protocol 2, the $M(H)$ loops

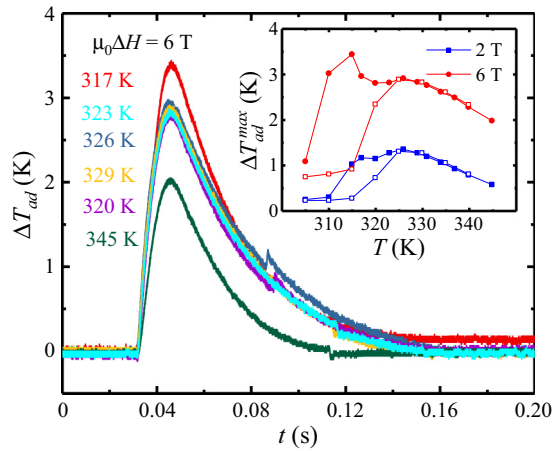


FIG. 2. Adiabatic temperature change, ΔT_{ad} , of $\text{Ni}_{2.2}\text{Mn}_{0.8}\text{Ga}$ as a function of time at a magnetic field of 6 T for different temperatures during cooling. Inset: $\Delta T_{\text{ad}}^{\text{max}}$ as a function of temperature for pulsed fields of 2 and 6 T. Open symbols represent data taken upon heating and closed upon cooling.

were recorded from 297 to 345 K, one after the other, without any thermal cycling as typically used for second-order phase transitions [see Fig. 1(c)] [30,31]. These $M(H)$ curves show that the transition from austenite to martensite can be induced at 323, 325, and 326 K using both protocols. However, there is no significant difference in the isothermal $M(H)$ curves recorded using the two different protocols. We further calculated magnetic entropy change (ΔS_M) from the isothermal $M(H)$ curves using the equation [31]

$$\Delta S_M = S(T, H) - S(T, 0) = \int_0^H \left(\frac{\partial M}{\partial T} \right)_H dH. \quad (1)$$

As expected, the $\Delta S_M(T)$ curves also show almost identical values for both protocols (heating) at all magnetic fields [see Fig. 1(d)]. However, we got a minor difference between both values at 300 K in a magnetic field of 1 T. This difference in the martensite phase can stem from a twinned structure of the martensite [32].

The small thermal hysteresis, reversibility in magnetization in the region of the martensitic transformation, and similar values of ΔS_M obtained for both protocols indicate that $\text{Ni}_{2.2}\text{Mn}_{0.8}\text{Ga}$ is a promising candidate for the observation of a reversible MCE and for future magnetocaloric applications. Therefore we investigated the MCE in details by direct measurements of ΔT_{ad} in pulsed magnetic fields. The pulsed magnetic field experiments provide the opportunity for an analysis of the temperature response of the material to magnetic field on a time scale of ~ 1 to 10 ms, which is comparable with typical operation frequencies (1 \sim 10 Hz) of magnetocaloric cooling devices [33]. The corresponding magnetic-field change rate is 2–50 T/s, in contrast to most studies reported in literature based on steady-field experiments with typical rates of 0.01 T/s. Thus pulsed-field studies provide a comprehensive access to the dynamics of the MCE near real operational conditions.

Figure 2 shows selected $\Delta T_{\text{ad}}(t)$ curves at different temperatures for magnetic field pulses of 6 T. All plotted data

were recorded after reaching the measurement temperatures during cooling from 350 K or from the previous measured temperature. Data on heating were also recorded (not shown here). ΔT_{ad} has contributions from both structural and magnetic transitions, similar to the case of $\text{Ni}_{2.19}\text{Mn}_{0.81}\text{Ga}$ where the transitions take place in the same temperature range [34]. It is important to note that for each of the temperatures $\Delta T_{\text{ad}}(t)$ goes back to the initial value before the pulse. This indicates the reversibility of the MCE. The inset of Fig. 2 displays $\Delta T_{\text{ad}}^{\text{max}}$, taken at the maximum in the $\Delta T_{\text{ad}}(t)$ curve, for applied magnetic fields of 2 and 6 T, recorded both on cooling and heating. For both fields, the broad shape of the maximum in the curves of $\Delta T_{\text{ad}}^{\text{max}}$, which is desirable for applications, covers a temperature window of about 35 K. Under a magnetic pulse of 6 T, $\Delta T_{\text{ad}}^{\text{max}}(t)$ reaches a maximum of 3.5 K at 317 K. We note, the directly measured value of $\Delta T_{\text{ad}}^{\text{max}}$ differs from that calculated from isothermal entropy change and specific heat data as expected and similar to previous studies on Ni_2MnGa and $\text{Ni}_{2.19}\text{Mn}_{0.81}\text{Ga}$ magnetic shape memory Heusler alloys [24,35–37].

To achieve higher efficiencies in magnetic cooling devices, the reversibility upon magnetic field cycling is crucial. To study the reversibility of the MCE in $\text{Ni}_{2.2}\text{Mn}_{0.8}\text{Ga}$, we have measured $\Delta T_{\text{ad}}(t)$ for three subsequent 6 T magnetic field pulses at 326 K reached upon cooling, which is just above the martensite start temperature, $M_s = 323$ K [see Fig. 3(a)]. Before pulse 1, the sample was heated to the austenite phase and subsequently cooled to the measurement temperature. Pulses 2 and 3 followed immediately after pulse 1. After pulse 1, $\Delta T_{\text{ad}}(t)$ exhibits an almost reversible behavior, only a small offset of 0.14 K remains. This value is almost unchanged for pulses 2 and 3. The $M(H)$ curve at 326 K shown in the inset of Fig. 3(a) clearly indicates the field induced transition from austenite to the martensite. We repeated the previously described experiment after further cooling down to 317 K. This temperature is in between the martensite start ($M_s = 323$ K) and martensite finish ($M_f = 315$ K) temperatures [see Fig. 3(b)]. After pulse 1, we found only a tiny irreversible offset of 0.26 K. After pulse 2, the offset of 0.13 K was even smaller, while the values of $\Delta T_{\text{ad}}^{\text{max}}$ for both pulses were almost the same. We note that the recorded offsets are smaller than the uncertainty in the measurement of ΔT [33]. Additionally, we investigated the irreversibility of the MCE at 329 K ($T > A_s$). Here, the measurement temperature was approached upon heating from well below the martensitic transition. At 329 K, four consecutive magnetic pulses up to 2 T were applied. As can be seen in Fig. 3(c), $\Delta T_{\text{ad}}(t)$ is reversible for all pulses. Thus, the previous results are a fair indication of the fast kinetics of the thermoelastic transformation, which is reversible due to the small hysteresis. Moreover, the pulsed magnetic field measurements give evidence that $\text{Ni}_{2.2}\text{Mn}_{0.8}\text{Ga}$ exhibits an almost perfect reversible MCE on the timescale of magnetocaloric devices.

In shape memory Heusler alloys, the occurrence of hysteresis, and consequently, an irreversible behavior of the MCE at the martensitic transformation, is closely related to the austenite and martensite phases and their interfaces. In most cases, this interface is a plane, known as habit plane. During the phase transformation from austenite to martensite, an elastic transition layer forms at the interface instead of an

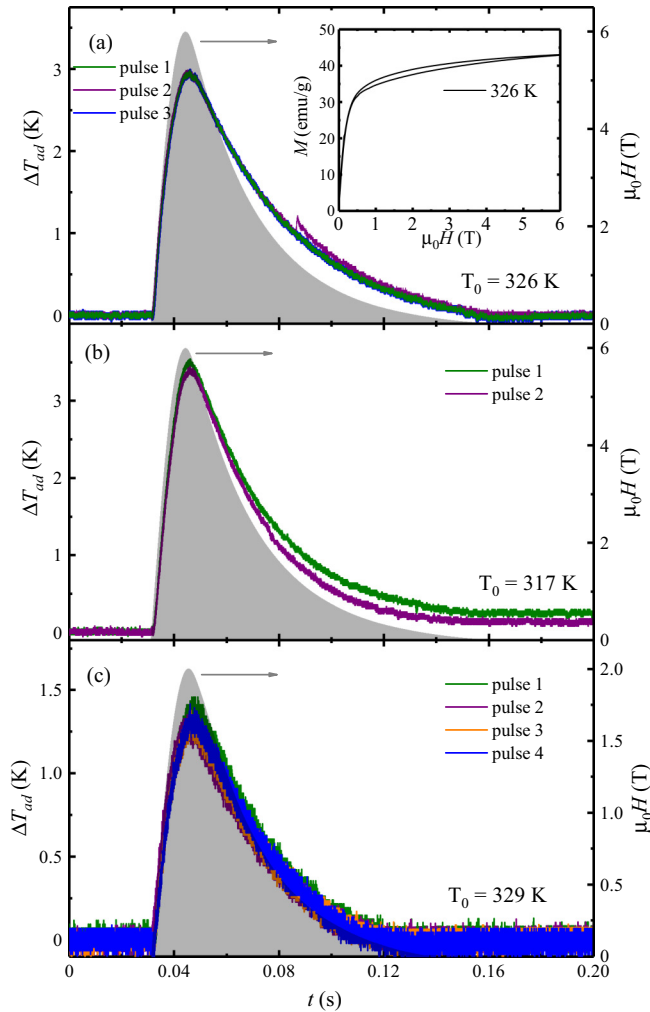


FIG. 3. Time dependence of ΔT_{ad} measured at (a) 326 and (b) 317 K reached upon cooling, for magnetic-field pulses of 6 T, and (c) at 329 K reached upon heating, for magnetic-field pulses of 2 T. See text for details. The right axes refer to the magnetic field profile. Inset in (a) shows the field induced $M(H)$ curve at 326 K after cooling the sample from 400 K.

exact interface between both phases. For forward and reverse transformation, the energy associated with the formation of an austenite/martensite interface results in hysteresis [20,38]. Recently, it has been shown that this hysteresis can be overcome by improving the compatibility condition between austenite and martensite phases [14,18–20]. The information about the compatibility of both phases is contained in the deformation matrix, which is calculated from the lattice parameters of both phases [18].

The martensitic transformation is diffusionless. The lattice vectors of both austenite and martensite phases are related by a homogenous 3×3 deformation matrix \mathbf{U} . This matrix \mathbf{U} is called Bain distortion matrix or the transformation matrix. The determinant of this matrix \mathbf{U} represents the volume change between the two phases. For the martensite and austenite phases to be compatible or for the formation of an exact interface between austenite and martensite, the determinant of the transformation matrix \mathbf{U} should be one. This

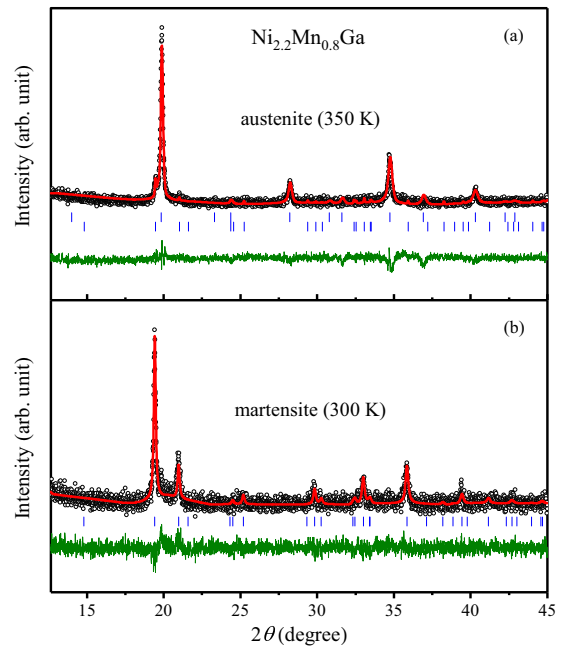


FIG. 4. LeBail refinements for PXRD patterns of $\text{Ni}_{2.2}\text{Mn}_{0.8}\text{Ga}$ in (a) austenite and (b) martensite phases. The experimental data are shown by circles and the fitted curve and residue by lines, respectively. The ticks represent Bragg-peak positions.

is called geometric compatibility condition for the material going from the cubic austenite to the martensite phase [18]. The transformation matrix \mathbf{U} and the number of modifications of martensite (tetragonal, monoclinic, and orthorhombic) vary for different systems [14,18,19].

To determine the transformation matrix \mathbf{U} for $\text{Ni}_{2.2}\text{Mn}_{0.8}\text{Ga}$, the structure information for both phases is needed. PXRD experiments were conducted at 350 and 300 K, to obtain data for the austenite and martensite phase. The LeBail fits of the PXRD patterns of both phases are shown in Fig. 4. At room temperature, $\text{Ni}_{2.2}\text{Mn}_{0.8}\text{Ga}$ is in martensitic phase ($M_s = 323$ K, see also Fig. 1). All of the reflections in the PXRD pattern could be indexed based on a body-centered tetragonal lattice (space group $I4/mmm$) and the lattice parameters were refined to $a = 3.9013(6)$ Å and $c = 6.5129(4)$ Å, while at 350 K $\text{Ni}_{2.2}\text{Mn}_{0.8}\text{Ga}$ is in the austenitic phase and has a cubic structure (space group $Fm\bar{3}m$). The refined lattice parameter is $a = 5.8286(2)$ Å. A small fraction of the martensite phase coexists at 350 K, which can be attributed to the effect of a residual stress generated upon grinding the ingot into powder [15–17].

In general, the cubic to tetragonal transformation can be described by two unequal stretches. The number of possible variants of martensite are determined by the number of rotations that are possible in the point group of the austenite P_a divided by the number of rotations that are possible in the point group of the martensite P_m . The number of rotations possible in the point group of the cubic austenite is 24, whereas the number of rotations possible in the point group of the martensite is 8. So, the cubic to tetragonal transformation results in three variants of martensite, which are, of course, related by symmetry and must have the same eigenvalue [23].

The variants of martensite for the face-centered cubic to face-centered tetragonal transformation are described as follows [18]:

$$\mathbf{U}_1 = \begin{pmatrix} \beta & 0 & 0 \\ 0 & \alpha & 0 \\ 0 & 0 & \alpha \end{pmatrix}, \mathbf{U}_2 = \begin{pmatrix} \alpha & 0 & 0 \\ 0 & \beta & 0 \\ 0 & 0 & \alpha \end{pmatrix},$$

and $\mathbf{U}_3 = \begin{pmatrix} \alpha & 0 & 0 \\ 0 & \alpha & 0 \\ 0 & 0 & \beta \end{pmatrix}.$ (2)

The transformational stretches α and β are derived from the lattice parameters of cubic austenite and face centered tetragonal martensite phases, $\alpha = \frac{a_F}{a_0}$ and $\beta = \frac{c_F}{a_0}$, where the index F stands for face centered. In our case, for a transformation from the face-centered cubic ($Fm\bar{3}m$) to the body-centered tetragonal ($I4/mmm$) structure, the lattice parameters of the body-centered unit cell can be converted to the face-centered unit cell by the following relationships: $a = a_F = \sqrt{2}a_I$ and $c = c_F = c_I$ [39]. Here, the index I stands for body centered. These stretches satisfy $\alpha > 0$, $\beta > 0$, and $\alpha \neq \beta$ [23].

Thus the transformation matrix of one of the corresponding martensite variants of $\text{Ni}_{2.2}\text{Mn}_{0.8}\text{Ga}$ is

$$\mathbf{U}_1 = \begin{pmatrix} 1.1174 & 0 & 0 \\ 0 & 0.9466 & 0 \\ 0 & 0 & 0.9466 \end{pmatrix}. \quad (3)$$

\mathbf{U}_2 and \mathbf{U}_3 follow directly from \mathbf{U}_1 according to Eq. (2). The determinant of this transformation matrix is very close to one, $|\mathbf{U}| = 1.0012$. The deviation from unity is only 0.12%, which is substantially smaller in comparison to the previous studies [39,40]. Mn_2NiGa exhibits a thermal hysteresis of 50 K [40]. From the lattice parameters, one obtains $|\mathbf{U}| = 0.9936$ with a variation of 0.64% from unity [40]. A slightly different composition, $\text{Ni}_{2.2}\text{Mn}_{0.75}\text{Ga}$, from our studied material, $\text{Ni}_{2.2}\text{Mn}_{0.8}\text{Ga}$, exhibits a hysteresis of 14 K in $|\mathbf{U}| = 0.9939$,

which differs 0.61% from unity [39]. These values deviate significantly more in comparison to our study. Hence exemplifying the validity of the geometric compatibility condition of the austenite and martensite phases in $\text{Ni}_{2.2}\text{Mn}_{0.8}\text{Ga}$.

In general, in shape memory Heusler alloys, the directly measured $\Delta T_{\text{ad}}(t)$ is expected to be influenced by the width of the hysteresis as well as the sharpness of the martensitic transition. Another factor that can also affect the reversibility of $\Delta T_{\text{ad}}(t)$ is a kinetic arrest due to a structurally and magnetically inhomogeneous state. In case of an alloy with a reduced hysteresis, the lattice coherence results in faster kinetics of the magnetostructural transformation and, thus, in a smaller energy barrier at the interface, consistent with our results.

In summary, we have studied the reversible adiabatic temperature change in the shape memory Heusler alloy $\text{Ni}_{2.2}\text{Mn}_{0.8}\text{Ga}$ and its relation to the structural properties at the martensitic transformation. We found that the reversibility of MCE is directly related to the small thermal and magnetic hysteresis, which is based on the geometric compatibility of the austenite and martensite phases in $\text{Ni}_{2.2}\text{Mn}_{0.8}\text{Ga}$. Therefore we can attribute the reversible behavior to the highly mobile transition layer between the two phases that leads to a reduction of the energy required for creating interfaces. Our finding provides a pathway to improve the reversibility of the MCE in shape memory Heusler alloys in the region of their martensitic transformation based on the geometric compatibility of the austenite and martensite phases.

This work was financially supported by the ERC Advanced Grant ‘TOPMAT’ (No. 742068). We acknowledge the support of the HLD at HZDR, member of the European Magnetic Field Laboratory (EMFL). S.S. thanks Alexander von Humboldt foundation, Germany and Science and Engineering Research Board of India for financial support through the award of Ramanujan Fellowship.

-
- [1] V. Franco, J. S. Blazquez, B. Ingale, and A. Conde, The magnetocaloric effect and magnetic refrigeration near room temperature: Materials and models, *Annu. Rev. Mater. Res.* **42**, 305 (2012).
- [2] E. Brück, Developments in magnetocaloric refrigeration, *J. Phys. D: Appl. Phys.* **38**, R381 (2005).
- [3] V. K. Pecharsky and K. A. Gschneidner, Giant Magnetocaloric Effect in $\text{Gd}_5(\text{Si}_2\text{Ge}_2)$, *Phys. Rev. Lett.* **78**, 4494 (1997).
- [4] J. D. Moore, K. Morrison, G. K. Perkins, D. L. Schlagel, T. A. Lograsso, K. A. Gschneidner, V. K. Pecharsky, and L. F. Cohen, Metamagnetism seeded by nanostructural features of single-crystalline $\text{Gd}_5(\text{Si}_2\text{Ge}_2)$, *Adv. Mater.* **21**, 3780 (2009).
- [5] A. Fujita, S. Fujieda, Y. Hasegawa, and K. Fukamichi, Itinerant-electron metamagnetic transition and large magnetocaloric effects in $\text{La}(\text{Fe}_x\text{Si}_{1-x})_{13}$ compounds and their hydrides, *Phys. Rev. B* **67**, 104416 (2003).
- [6] F. X. Hu, B. G. Shen, J. R. Sun, Z. H. Cheng, G. H. Rao, and X. X. Zhang, Influence of negative lattice expansion and metamagnetic transition on magnetic entropy change in the compound $\text{LaFe}_{1.4}\text{Si}_{1.6}$, *Appl. Phys. Lett.* **78**, 3675 (2001).
- [7] J. Lyubina, K. Nenkov, L. Schultz, and O. Gutfleisch, Multiple Metamagnetic Transitions in the Magnetic Refrigerant $\text{La}(\text{Fe}, \text{Si})_{13}\text{H}_x$, *Phys. Rev. Lett.* **101**, 177203 (2008).
- [8] H. Wada, K. Taniguchi, and Y. Tanabe, Extremely large magnetic entropy change of $\text{MnAs}_{1-x}\text{Sb}_x$ near room temperature, *Mater. Trans.* **43**, 73 (2002).
- [9] O. Tegus, E. Brück, K. H. J. Buschow, and F. R. de Boer, Transition-metal-based magnetic refrigerants for room-temperature applications, *Nature (London)* **415**, 150 (2002).
- [10] J. Du, Q. Zheng, W. J. Ren, W. J. Feng, X. G. Liu, and Z. D. Zhang, Magnetocaloric effect and magnetic-field-induced shape recovery effect at room temperature in ferromagnetic heusler alloy Ni-Mn-Sb, *J. Phys. D: Appl. Phys.* **40**, 5523 (2007).
- [11] T. Krenke, M. Acet, E. F. Wassermann, X. Moya, L. Mañosa, and A. Planes, Inverse magnetocaloric effect in ferromagnetic Ni-Mn-Sn alloys, *Nat. Mater.* **4**, 450 (2005).

- [12] M. Ghorbani Zavareh, C. Salazar Mejía, A. K. Nayak, Y. Skourski, J. Wosniza, C. Felser, and M. Nicklas, Direct measurements of the magnetocaloric effect in pulsed magnetic fields: The example of the Heusler alloy $\text{Ni}_{50}\text{Mn}_{35}\text{In}_{15}$, *Appl. Phys. Lett.* **106**, 071904 (2015).
- [13] J. Liu, T. Gottschall, K. P. Skokov, J. D. Moore, and O. Gutfleisch, Giant magnetocaloric effect driven by structural transitions, *Nat. Mater.* **11**, 620 (2012).
- [14] Y. Song, X. Chen, V. Dabade, T. W. Shield, and R. D. James, Enhanced reversibility and unusual microstructure of a phase-transforming material, *Nature (London)* **502**, 85 (2013).
- [15] S. Singh, P. Kushwaha, F. Scheibel, H. P. Liermann, S. R. Barman, M. Acet, C. Felser, and D. Pandey, Residual stress induced stabilization of martensite phase and its effect on the magnetocaloric effect in Mn-rich Ni-Mn-In/Ga magnetic shape memory alloys, *Phys. Rev. B* **92**, 020105 (2015).
- [16] S. Singh, J. Nayak, A. Rai, P. Rajput, A. H. Hill, S. R. Barman, and D. Pandey, (3+1)d superspace description of the incommensurate modulation in the premartensite phase of Ni_2MnGa : A high resolution synchrotron x-ray powder diffraction study, *J. Phys.: Condens. Matter* **25**, 212203 (2013).
- [17] S. Singh, V. Petricek, P. Rajput, A. H. Hill, E. Suard, S. R. Barman, and D. Pandey, A high resolution synchrotron x-ray powder diffraction study of the incommensurate modulation in the premartensite phase of Ni_2MnGa : Evidence for nearly 7M modulation and phason broadening, *Phys. Rev. B* **90**, 014109 (2014).
- [18] Kaushik Bhattacharya, *Microstructure of Martensite: Why it Forms and how it Gives Rise to the Shape Memory Effect*, edited by Adrian P. Sutton and Robert E. Rudd, Oxford Series on Materials Modelling (Oxford University Press Inc., New York, 2003).
- [19] J. Cui, Y. S. Chu, O. O. Famodu, Y. Furuya, J. Hattrick-Simpers, R. D. James, A. Ludwig, S. Thienhaus, M. Wuttig, Z. Zhang, and I. Takeuchi, Combinatorial search of thermoelastic shape memory alloys with extremely small hysteresis width, *Nat. Mater.* **5**, 286 (2006).
- [20] V. Srivastava, X. Chen, and R. D. James, Hysteresis and unusual magnetic properties in the singular Heusler alloy $\text{Ni}_{45}\text{Co}_5\text{Mn}_{40}\text{Sn}_{10}$, *Appl. Phys. Lett.* **97**, 014101 (2010).
- [21] R. D. James and K. F. Hane, Martensitic transformations and shape memory materials, *Acta Mater.* **48**, 197 (2000).
- [22] Z. Zhang, R. D. James, and S. Müller, Energy barriers and hysteresis in martensitic phase transformations, *Acta Mater.* **57**, 4332 (2009).
- [23] K. F. Hane and T. W. Shield, Symmetry and microstructure in martensites, *Phil. Mag. A* **78**, 1215 (1998).
- [24] V. V. Khovaylo, K. P. Skokov, Yu. S. Koshkid'ko, V. V. Koledov, V. G. Shavrov, V. D. Buchelnikov, S. V. Taskaev, H. Miki, T. Takagi, and A. N. Vasiliev, Adiabatic temperature change at first-order magnetic phase transitions: $\text{Ni}_{2.19}\text{Mn}_{0.81}\text{Ga}$ as a case study, *Phys. Rev. B* **78**, 060403(R) (2008).
- [25] V. V. Khovailo, T. Takagi, J. Tani, R. Z. Levitin, A. A. Cherechukin, M. Matsumoto, and R. Note, Magnetic properties of $\text{Ni}_{2.18}\text{Mn}_{0.82}\text{Ga}$ Heusler alloys with a coupled magnetocaloric transition, *Phys. Rev. B* **65**, 092410 (2002).
- [26] V. V. Khovaylo, T. Kanomata, T. Tanaka, M. Nakashima, Y. Amako, R. Kainuma, R. Y. Umetsu, H. Morito, and H. Miki, Magnetic properties of $\text{Ni}_{50}\text{Mn}_{34.8}\text{In}_{15.2}$ probed by Mössbauer spectroscopy, *Phys. Rev. B* **80**, 144409 (2009).
- [27] T. Gottschall, K. P. Skokov, B. Frincu, and O. Gutfleisch, Large reversible magnetocaloric effect in Ni-Mn-In-Co, *Appl. Phys. Lett.* **106**, 021901 (2015).
- [28] J. Liu, N. Scheerbaum, J. Lyubina, and O. Gutfleisch, Reversibility of magnetocaloric transition and associated magnetocaloric effect in Ni-Mn-In-Co, *Appl. Phys. Lett.* **93**, 102512 (2008).
- [29] T. Gottschall, K. P. Skokov, R. Burriel, and O. Gutfleisch, On the S (T) diagram of magnetocaloric materials with first-order transition: Kinetic and cyclic effects of Heusler alloys, *Acta Materialia* **107**, 1 (2016).
- [30] V. K. Pecharsky and K. A. Gschneidner, Magnetocaloric effect from indirect measurements: Magnetization and heat capacity, *J. Appl. Phys.* **86**, 565 (1999).
- [31] S. Singh, S. W. D'Souza, K. Mukherjee, P. Kushwaha, S. R. Barman, S. Agarwal, P. K. Mukhopadhyay, A. Chakrabarti, and E. V. Sampathkumaran, Magnetic properties and magnetocaloric effect in Pt doped Ni-Mn-Ga, *Appl. Phys. Lett.* **104**, 231909 (2014).
- [32] A. Planes, L. Mañosa, and M. Acet, Magnetocaloric effect and its relation to shape-memory properties in ferromagnetic Heusler alloys, *J. Phys.: Condens. Matter* **21**, 233201 (2009).
- [33] M. Ghorbani Zavareh, Direct measurements of the magnetocaloric effect in pulsed magnetic fields, Ph.D. thesis, Technical university of Dresden, 2016.
- [34] L. Pareti, M. Solzi, F. Albertini, and A. Paoluzi, Giant entropy change at the co-occurrence of structural and magnetic transitions in the $\text{Ni}_{2.19}\text{Mn}_{0.81}\text{Ga}$ Heusler alloy, *Eur. Phys. J. B* **32**, 303 (2003).
- [35] L. Mañosa, A. Gonz'alez-Comas, E. Obradó, A. Planes, V. A. Chernenko, V. V. Kokorin, and E. Cesari, Anomalies related to the TA_{2-} phonon-mode condensation in the Heusler Ni_2MnGa alloy, *Phys. Rev. B* **55**, 11068 (1997).
- [36] M. R. Kirkham, High temperature specific heat capacity measurement of $\text{Ni}_{2+x}\text{Mn}_{1-x}\text{Ga}$, Ph.D. thesis, Loughborough University, 2014.
- [37] C. P. Sasso, M. Pasquale, L. Giudici, S. Besseghini, and E. Villa, Magnetocaloric transitions and adiabatic temperature variation in polycrystal and single-crystal Ni_2MnGa alloys, *J. Appl. Phys.* **99**, 08K905 (2006).
- [38] R. Zarnetta, T. Takahashi, M. L. Young, A. Savan, Y. Furuya, S. Thienhaus, B. Maaß, M. Rahim, J. Frenzel, H. Brunken, Y. S. Chu, V. Srivastava, R. D. James, I. Takeuchi, G. Eggeler, and A. Ludwig, Identification of quaternary shape memory alloys with near-zero thermal hysteresis and unprecedented functional stability, *Adv. Funct. Mater.* **20**, 1917 (2010).
- [39] S. Banik, R. Ranjan, A. Chakrabarti, S. Bhardwaj, N. P. Lalla, A. M. Awasthi, V. Sathe, D. M. Phase, P. K. Mukhopadhyay, D. Pandey, and S. R. Barman, Structural studies of $\text{Ni}_{2+x}\text{Mn}_{1-x}\text{Ga}$ by powder x-ray diffraction and total energy calculations, *Phys. Rev. B* **75**, 104107 (2007).
- [40] G. D. Liu, J. L. Chen, Z. H. Liu, X. F. Dai, G. H. Wu, B. Zhang, and X. X. Zhang, Martensitic transformation and shape memory effect in a ferromagnetic shape memory alloy: Mn_2NiGa , *Appl. Phys. Lett.* **87**, 262504 (2005).